NeuroImage 216 (2020) 116522

Contents lists available at ScienceDirect

NeuroImage

journal homepage: www.elsevier.com/locate/neuroimage

Dissociable neural systems for unconditioned acute and sustained fear

Matthew Hudson [a,*], Kerttu Seppälä [a], Vesa Putkinen [a], Lihua Sun [a], Enrico Glerean [b], Tomi Karjalainen [a], Henry K. Karlsson [a], Jussi Hirvonen [c], Lauri Nummenmaa [a,d]

[a] Turku PET Centre, University of Turku, Turku, Finland
[b] Department of Neuroscience and Biomedical Engineering, School of Science, Aalto University, Espoo, Finland
[c] Department of Radiology, Turku University Hospital, Turku, Finland
[d] Department of Psychology, University of Turku, Turku, Finland

ARTICLE INFO

Keywords:
Fear
Threat
Neural synchronization
Horror movies
Naturalistic fMRI

ABSTRACT

Fear protects organisms by increasing vigilance and preparedness, and by coordinating survival responses during life-threatening encounters. The fear circuit must thus operate on multiple timescales ranging from preparatory sustained alertness to acute fight-or-flight responses. Here we studied the brain basis of sustained and acute fear using naturalistic functional magnetic resonance imaging (fMRI) enabling analysis of different time-scales of fear responses. Subjects (N = 37) watched feature-length horror movies while their hemodynamic brain activity was measured with fMRI. Time-variable intersubject correlation (ISC) was used to quantify the reliability of brain activity across participants, and seed-based phase synchronization was used for characterizing dynamic connectivity. Subjective ratings of fear were used to assess how synchronization and functional connectivity varied with emotional intensity. These data suggest that acute and sustained fear are supported by distinct neural pathways, with sustained fear amplifying mainly sensory responses, and acute fear increasing activity in brainstem, thalamus, amygdala and cingulate cortices. Sustained fear increased ISC in regions associated with acute fear, and also amplified functional connectivity within this network. The results were replicated in an independent experiment with a different subject sample and stimulus movie. The functional interplay between cortical networks involved in sustained anticipation of, and acute response to, threat involves a complex and dynamic interaction that depends on the proximity of threat, and the need to employ threat appraisals and vigilance for decision making and response selection.

1. Introduction

Emotions prepare us for action. They motivate seeking out rewarding stimuli, increasing alertness and avoiding threat (Bernhardt and Singer, 2012). Fear has a strong developmental and evolutionary function as a primordial reaction to danger that elicits a distinctive physiological and psychological response. The endocrine system releases epinephrine, norepinephrine, and cortisol that excites the cardiovascular and respiratory systems, and releases glucose into the bloodstream, preparing the body for physical action (Rodrigues et al., 2009). A concomitant increase in attentional vigilance (Finucane, 2011) and a bias toward threatening stimuli (Öhman et al., 2001) serve to heighten perceptual awareness, and learning/memory mechanisms (Öhman and Mineka, 2001). Fear is associated with changes in both the central and peripheral nervous system (Ekman, 1992; Kreibig, 2010; Nummenmaa and Saarimäki, 2017; Panksepp, 1982) and is also characterized by an idiosyncratic subjective experience (Nummenmaa et al., 2014a,b; Nummenmaa et al., 2018a,b; Volynets et al., 2019) and overt expression (Smith et al., 2005).

Acute fear in response to encountering threat is associated with a distinctive pattern of neural activity distributed through the cerebellum (Ploghaus et al., 1999), limbic system (Knight et al., 2004; LaBar et al., 1998), and cortex (*prefrontal:* Phelps, Delgado, Nearing and LeDoux, 2004; *sensory:* Morris et al., 2001; *cingulate:* Milad et al., 2007; *insula:* Critchley et al., 2002; *motor:* Lissek et al., 2014). This distributed network (Saarimäki et al., 2016) enables the rapid detection and appraisal of threat, its saliency to oneself, the employment of executive functioning and memory for decision making and action planning, and the implementation of action plans (Zhu and Thagard, 2002).

In addition to generating immediate survival responses, fear systems also modulate vigilance in anticipation of threat caused by environmental cues, perceptual uncertainty, and ambiguity that elicits a sustained fear prior to actual encountering of threat (Fanselow, 1994; Lang

* Corresponding author. National College of Ireland, School of Business, National College of Ireland, Mayor Street IFSC, Dublin 1, Ireland.
E-mail address: matthew.hudson@ncirl.ie (M. Hudson).

https://doi.org/10.1016/j.neuroimage.2020.116522
Received 23 October 2019; Received in revised form 19 December 2019; Accepted 3 January 2020
Available online 8 January 2020

et al., 2000; Lehne and Koelsch, 2015). This gives rise to subjective feelings of anxiety, tension, suspense, dread, or foreboding that reflects a generalized anticipatory preparedness for the possibility of potential danger. Several recent studies have shown that spatiotemporally distant threats elicit activity in the ventromedial prefrontal cortex, posterior cingulate cortex, hippocampus and amygdala, which are associated with a cognitive mechanism of fear that reflects the need for complex information processing and memory retrieval to generate an adaptive and flexible response. A threat that is proximal in space or time, on the other hand, elicits a reactive fear response of immediate action and fight or flight, and which elicits activity in the periaqueductal gray, amygdala, hypothalamus, and middle cingulate cortex (Mobbs et al., 2007; Qi et al., 2018).

To date, several studies have employed naturalistic stimuli, such as horror movie clips (e.g., Kinreich et al., 2011), or dynamically interacting with a virtual predator (Mobbs et al., 2007; Qi et al., 2018), to establish the differential cortical activity implicated in sustained and acute fear. However, they employed a discrete and categorical distinction of pre or post threat onset, thus failing to capture the temporal dynamics and fluctuation of the fear response. Therefore, the neural mechanisms supporting dynamically fluctuating and sustained fear, versus acute fear responses, during naturalistic conditions remains poorly characterized. Furthermore, the majority of human neuroimaging studies have been conducted using relatively impoverished and reduced laboratory settings, which does not necessarily provide an optimal model of how the brain responds to survival challenges in the real world (see review in Adolphs et al., 2016). First, the brain has evolved to parse the dynamic world and its complex events, and it is known that neural responses to complex stimuli cannot necessarily be predicted on the statistical combination of responses to simple stimuli (Felsen and Dan, 2005). During evolution the brain has been tuned to respond to a complex and continuously changing world rather than to static and isolated signals. Accordingly, cells in the cat visual cortex show stronger responses to real pictures than to random patterns (Touryan et al., 2005), and gamma band responses and local field potentials are also most reliable in response to repeated presentations of movies (Belitski et al., 2008). In humans, life-like moving faces also elicit markedly stronger activation in the face processing network than static or rigidly moving faces (Fox et al., 2009; Schultz et al., 2013). And most importantly, many psychological phenomena – including fear – span multiple overlapping time scales and parallel processing of multiple features, thus they cannot be adequately studied with rigid and tightly controlled classical experimental designs.

Recent advances in brain signal analysis have however enabled characterization of brain activity during naturalistic and unconstrained conditions where the stimulus space is high-dimensional (Nummenmaa et al., 2018a,b). During natural audiovisual stimulation, subjects' brain activation becomes synchronized in occipital and temporal regions of the cortex, due to the identical perceptual experience of the participants (Glerean et al., 2012; Hasson et al., 2004). The spatial distribution of the synchronization is functionally specific: for example, greater synchronization in the fusiform gyrus is found during portions of the movie when faces are visible (Hasson et al., 2008). Such neural synchronization is subject not only to bottom-up changes in perceptual input but top-down changes in attentional control (Lahnakoski et al., 2014). Importantly, activity in regions involved in the perception and experience of emotions become increasingly synchronized across individuals as a function of the emotional content of the stimulus (Nummenmaa et al., 2012; Nummenmaa et al., 2014a, 2014b). For example, changes of emotional valence from positive to negative alters synchronization in regions such as the thalamus, anterior cingulate cortex, and prefrontal cortex. In contrast, the arousal elicited by an emotional stimulus alters synchronization in visual and somatosensory regions (Nummenmaa et al., 2012, 2014b). These methods can capture the complex temporal dynamics of neural activity in response to naturalistic stimuli for which controlled modelling is not possible, but nevertheless reveal reliable neural activity at the population level on a moment-to-moment basis in functionally specific brain regions.

Additionally, the prolonged and variable brain activation time series resulting from naturalistic stimulation is well-suited for analyzing dynamic connectivity changes (Nummenmaa et al., 2014b). Prior studies on emotion-dependent brain connectivity have typically constrained the analysis to a small numbers of regions of interest and suffered from the low power of conventional event-related and boxcar designs in connectivity analyses (e.g. Eryilmaz et al., 2011; Passamonti et al., 2008; Tettamanti et al., 2012). A naturalistic stimulation setup in turn offers a high-powered alternative for tapping fear-dependent connectivity in the brain.

1.1. The present study

The aim of the current study was to investigate, in naturalistic settings, the neural mechanisms involved in generating acute fear responses after threat onset and those supporting sustained anticipatory fear when the threat is not yet present. Subjects viewed feature-length horror movies while their brain activity was recorded with fMRI. Acute threatening events ("jump-scares") were annotated in the movies, and self-reports of sustained fear were obtained. These time series were subsequently used for predicting hemodynamic activity, voxel-wise intersubject correlation, and functional connectivity. We show that acute and sustained fear are supported by distinct neural pathways. Importantly, we confirm the consistency of these effects using a voxel-wise intraclass-correlation reliability measure across two independent data sets with different subjects and stimuli.

2. Materials and methods

The study protocol was approved by the ethics board of the hospital district of Southwest Finland, and the study was conducted in accordance with the Declaration of Helsinki.

2.1. Stimuli

Two feature length horror movies (The Conjuring 2, 2016, and Insidious, 2010; both directed by James Wan) were selected based on a pilot survey on horror movies. Online databases (Rotten Tomatoes, International Movie Database, AllMovie) were consulted to generate a list of the 100 best-rated horror movies of the past 100 years (see **Supplementary Materials**). An independent sample of 216 participants completed a survey asking if they had seen the movies and, if so, rated them on scariness and quality. The participants also reported how often they watched horror movies or movies in general, and how scary they considered different types of horror (e.g. psychological horror, supernatural horror). Finally, the participants reported the most common emotions experienced while viewing horror movies. These data (Fig. 1) confirmed that viewing horror movies was common, a total of 72% of respondents reported watching at least one horror movie every six months. Psychological horror and movies based on supernatural as well as real events were rated as most frightening and viewing horror movies was associated with the targeted emotions (fear, anxiety, excitement). Data for the exposure, and fear and quality ratings for the top ten scariest movies are shown in Table 1 (see **Supplementary Analysis 3** for the full results). Scariness and quality ratings (Bonferroni corrected alpha = 0.017) were positively correlated ($r = .528$, $p < .001$) showing that movies considered as high quality were also considered as scary.

The selected movies were chosen on the basis of this survey as 1) they were rated highly for scariness (Conjuring 2 = 7.0; Insidious = 7.1) and quality (Conjuring 2 = 7.3; Insidious = 7.1), and 2) relatively few people had seen them (Conjuring 2 = 17.4%; Insidious = 13.5%). Each movie had a high number of abrupt threat onsets ("jump-scares": Conjuring 2 n

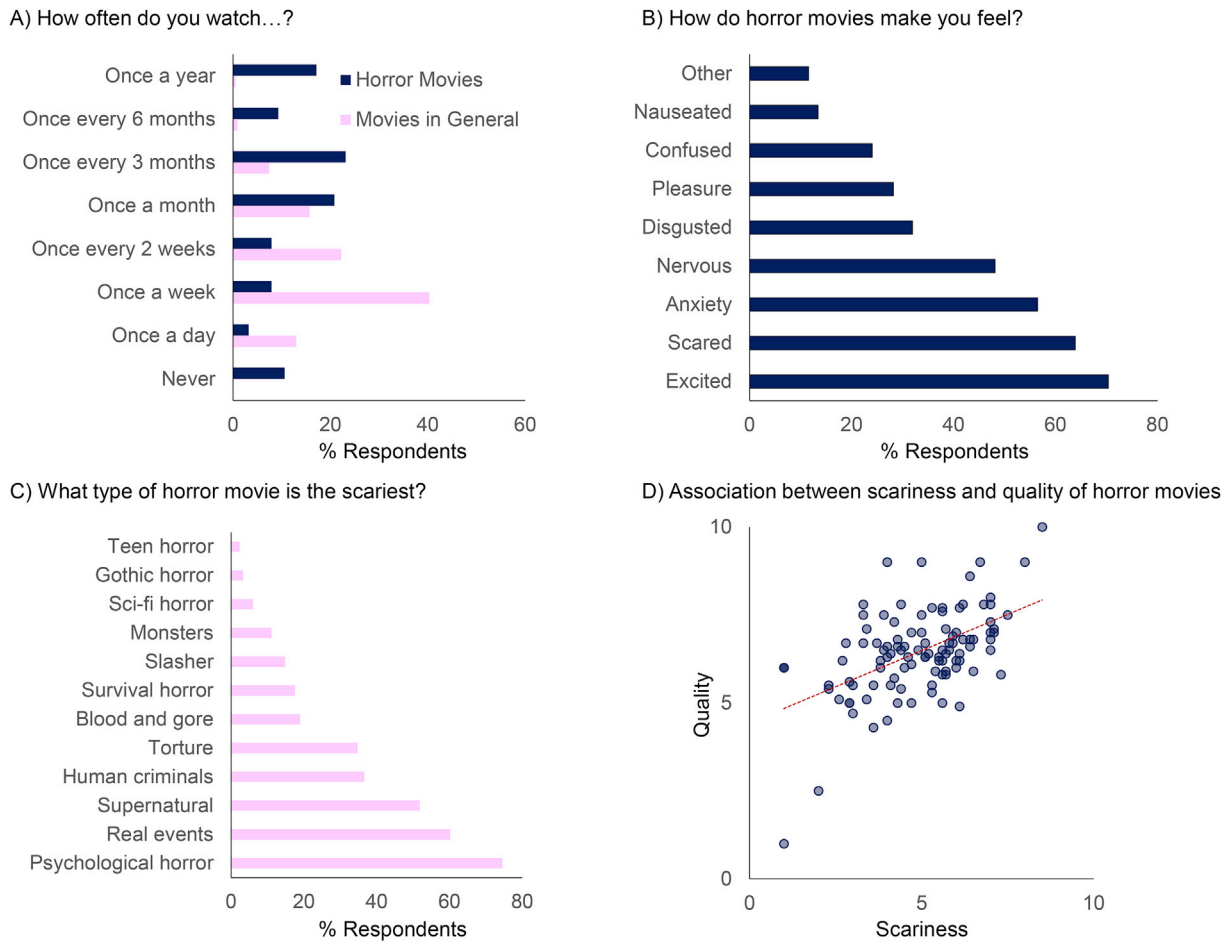

Fig. 1. Emotional responses to horror movies. The frequency of viewing horror movies by the sample (A), and the different emotions experienced while viewing horror movies (B), as well as the type of horror movie that participants found to be the scariest (C). Lastly, the relationship between the scariness of the horror movie and its quality (D).

Table 1
Top ten scariest movies in the survey. Title and year of release, alongside familiarity with the film, and scariness and quality ratings by those who had seen it, and also the number of jump-scares (where available). Selected movies indicated in bold.

		Have you seen this movie?					
Title	Year	Yes	No, but heard of it	Not seen nor heard of it	Scary	Quality	Jump scares
The Devil's Backbone	2001	4.2	6.3	89.6	8.5	10.0	4
The Wailing	2016	2.1	8.3	89.6	8.0	9.0	4
The Conjuring	2013	39.6	31.3	29.2	7.5	7.5	12
REC 2	2009	10.4	29.2	60.4	7.3	5.8	–
Insidious	**2010**	**29.2**	**25.6**	**45.2**	**7.1**	**7.1**	**24**
The Exorcist	1973	53.0	23.2	23.8	7.1	7.0	10
Goodnight Mommy	2015	4.2	10.4	85.4	7.0	8.0	1
A Chinese Ghost Story	1987	1.8	7.1	91.1	7.0	7.8	–
The Conjuring 2	**2016**	**37.5**	**31.0**	**31.5**	**7.0**	**7.3**	**22**
Under The Shadow	2016	2.1	14.6	83.3	7.0	7.0	9

Table 2
Stimulus segment durations (mins:secs) and the scanning run in which they were presented.

	Run 1		Run 2		Run 3		Run 4		Total
Conjuring 2	15:33	13:33	10:55	07:25	11:41	14:46	10:51	10:31	14:02	109m 17s
Insidious	16:00	15:16	14:49	10:59	07:53	14:34	15:04	–	–	94m 35s

= 22; Insidious n = 24), which were indexed from an online database (http://wheresthejump.com, 2017, see **Supplementary Materials**). Each movie was edited for length (see **Supplementary Materials**) with Apple iMovie whilst maintaining the fear elements of the film. The movies were split into short segments to optimize stimulus delivery and data processing (see Table 2.), and to allow short breaks for the subjects. Cut-points adhered to naturally occurring scene transitions within the films. The videos were presented at 23.98fps at a resolution of 800 * 600.

2.2. Participants

A total of 51 subjects took part in the brain imaging and behavioral experiments (mean age = 24.5, SD = 5.5, 30 females). Imaging data were obtained from 37 participants (Conjuring 2: n = 18, Insidious: n = 19). One further subject was scanned (The Conjuring 2) but the scan had to be terminated due to subject discomfort. Twenty-five of these participants also provided behavioral ratings for one of the movies. An additional 14 participants were recruited to provide behavioral ratings only (three for both movies, four for Conjuring 2, seven for Insidious, although one participant who rated both movies was excluded for not complying to task instructions), leaving n = 20 for both movies. No participant viewed the same movie twice (See Table 3 for details). Subjects were recruited from the University of Turku and surrounding community, they received payment and/or course credit as compensation, and provided written informed consent prior to taking part. No participants had a history of neuropsychiatric symptoms or medication.

2.3. Procedure

Behavioral Fear Ratings: Subjects viewed the movie on an iMac retina 5K 27-inch monitor running High Sierra 10.13.3. Audio was delivered via AKG K550 MKII headphones (32 Ω, 114 db, 12hz to 28 kHz). A vertically oriented slider ranging from zero (no fear) to one (maximum fear) was placed to the right of the movie window. Participants controlled the location of a cursor on the scale by moving it upwards (push the mouse forward) when their fear increased and moving the cursor downwards (pull the mouse backward) when their fear decreased. The cursor position was monitored at 5 Hz. Subjects were told to use the full range of the scale and to make sure that their rating continuously reflected how scared they were. Stimuli were presented as segments, and a timer was placed inconspicuously at the top of the screen that counted down until the end of the current segment. Participants were told that they were free to take a break but that they should wait until the end of the current segment before they did so.

fMRI Acquisition and Pre-processing: MR imaging was conducted at Turku PET Centre at the University of Turku using a Philips Ingenuity TF 3-Tesla scanner. Anatomical images (1 mm^3 resolution) were acquired using a T1-weighted sequence (1 mm^3 resolution, TR 8.1 ms, TE 3.7 ms, flip angle 7°, 256 mm FOV, 256 × 256 acquisition matrix, 176 sagittal slices). Whole-brain functional data were acquired with T2*-weighted echo-planar imaging sequence, sensitive to the blood-oxygen-level-dependent (BOLD) signal contrast (TR = 2600 ms, TE = 30 ms, 75° flip angle, 250 mm FOV, 80 × 80 acquisition matrix, 53.4 Hz bandwidth, 3.0 mm slice thickness, 45 interleaved slices acquired in ascending order without gaps).

Scanning was split into short runs of approximately 25 min each (see Table 2.) for the sake of subject comfort (number of volumes: The Conjuring 2, 675, 696, 595, and 572 vol (total 2538 scans); Insidious: 725, 780, and 687 vol (total 2192 scans)) with breaks between each run. Stimulus video was displayed using goggles affixed to the head coil (NordicNeuroLab VisualSystem). Audio was played through SensiMetrics S14 earphones (100 Hz–8 kHz bandwidth, 110 dB SPL). Volume was adjusted to a comfortable level that could still be heard over the scanner noise.

Table 3
Distribution of subjects for whom imaging data and/or behavioral fear ratings were acquired across the two movies (prior to subject exclusions).

Movie		The Conjuring 2			
		Scan	Rate	Not Viewed	Total
Insidious	Scan	1	14	4	19
	Rate	11	3	7	21
	Not Viewed	7	4	–	11
	Total	19	21	11	51

Functional data were preprocessed with FSL (www.fsl.fmrib.ox.ac.uk) using the FEAT pipeline. The EPI images were realigned to the middle scan by rigid body transformations to correct for head movements (six parameters). Two-step coregistration was conducted firstly to the participant's T1 weighted structural image, and secondly to MNI152 2 mm template. Spatial smoothing used isotropic Gaussian Kernel with 8 mm FWHM (Pajula and Tohka, 2014). Low-frequency drifts in data were estimated and removed using a 240s Savitzky-Golay filter (Çukur et al., 2013). To control for motion artefacts, motion related regressors were added as nuisance regressors following Power et al. (2012).

2.4. Data analysis

2.4.1. General Linear Model Analysis

GLM analyses were implemented with SPM 12 (www.fil.ion.ucl.ac.uk/spm) with a two-stage random effects analysis. All results were thresholded with a cluster-level FWE corrected alpha of 0.001, unless noted otherwise, and an extent threshold of ten voxels to remove isolated significant voxels. Frame-wise luminance and sound intensity time series were derived using custom Matlab toolbox and down-sampled to 2.6 s (1 TR). As these low-level stimulus features correlated with behavioral fear ratings (see Results), they inevitably covaried with the BOLD signal of interest. In a supplementary analyses (Supplementary Figs. 3A and 3B), luminance and sound intensity were entered as nuisance regressors in all analyses; however, they did not alter the results appreciably. All results in the main analysis are therefore reported without these regressors. Primary second-level analyses were conducted together for both movies, with separate analyses reported in the Supplementary Materials. Physiological data was not collected, as previous fMRI studies have revealed that physiological responses only weakly correlate with subjective emotional measures in this kind of paradigm (Nummenmaa et al., 2014b; Smirnov et al., 2019).

Jump-scares: We first modelled the brain responses to acute fear onsets. In the first-level analysis we modelled jump-scares with stick functions convolved with a canonical hemodynamic response function. High-pass filter period was set to 128s. Second-level analysis (random-effects) was conducted on the resulting contrasts using a one sample *t*-test.

Dynamic Fear Ratings: Sustained fear responses were analyzed using the behavioral fear ratings averaged across subjects. In the first-level analysis, the TR down-sampled fear ratings were convolved with a canonical hemodynamic response function and entered as a regressor into the GLM analysis, using a high-pass filter of 256s to reflect the slower frequency of the fear ratings (see also Nummenmaa et al., 2014b). The contrast images generated in the first-level models were then subjected to second-level (random effects) testing with one-sample *t*-test.

Intraclass correlation: The study design provided an opportunity to investigate if the observed effects replicated across different samples in response to different stimulus movies. To provide a statistical estimate of reliability, intraclass correlation (ICC) analyses were conducted across the two samples (see Bennett and Miller, 2010; Chen et al., 2017). A one-way random effects between-subjects ICC (1,1) (Shrout and Fleiss, 1979) was conducted for each voxel. The t-contrast for each participant at the first level of analysis was subject to a one-way between subjects ANOVA, and the between subjects (BS) and within subjects (WS) mean square (MS) was used to compute the ICC by dividing the target variance (BS_MS − WS_MS) over the total variance (BS_MS + (2*WS_MS)). The variance ratio varies between zero and one, with higher values reflecting greater reliability (Koo and Li, 2016). The ICC maps for the jump-scares and dynamic fear ratings are presented in the Supplementary Materials.

2.4.2. Inter-Subject Correlation Analysis (ISC)

ISC provides a model-free means for analyzing hemodynamic responses to complex naturalistic stimuli (Hasson et al., 2004). ISC was implemented using the ISC toolbox (release 21: https://www.nitrc.org/projects/isc-toolbox/). Detailed information can be found at Kauppi et al. (2014). Pearson correlation coefficient for each subject pair voxel

time series provided a measure of across subject similarity in BOLD activity.

ISC was calculated in two ways. First, mean ISC was computed for the full time series to provide an average ISC map during the course of the whole movie. Briefly, a participant-wise correlation matrix was conducted for each voxel time series. The array of r values was Fisher z transformed to make them normally distributed and amenable for statistical analysis. The values were averaged and index the degree of neural synchronization for each voxel. The higher the value, the more similar and less variable the time series of neural activity is across participants. This reveals the typical time-locking of neural responses across subjects throughout the movie. Statistical significance of the ISC values was calculated by means of a fully nonparametric voxel-wise permutation test of the r value. Each subject's time series was circularly shifted by a random number of time points, which preserved the temporal autocorrelations present within each time series but disrupted the temporal alignment between subjects. The ISC value was computed over 1,000,000 realizations, and the resulting distribution of r values represent the non-correlated time series that would be expected if the null hypothesis were true, and from which the population ISC would be derived if there were no reliability between subjects. The p values were FDR thresholded at $p = 0.05$ without assumptions.

Second, a dynamic measure of neural synchronization was calculated to establish how intersubject synchronization varies throughout the movie. Such a dynamic approach allows modelling of whether moment-to-moment ISC is associated with the behavioral measure of sustained fear. Voxel-wise ISC values were computed for each time point with a sliding window of ten samples (see Nummenmaa et al., 2012). Dynamic ISC time series were computed separately for each session. As each session lost nine time points due to the sliding window, the voxel time-series were de-meaned and the sliding window ISC was calculated for the concatenated final nine volumes of one session and the first nine volumes of the next session, producing the ISC for the missing nine time points. This provided a continuous ISC measure across the whole movie (minus the final nine samples). Fear ratings (down-sampled to 1 TR) were also subjected to similar moving averaging with a ten sample sliding window to match their temporal resolution with the dynamic ISC signal. The fear ratings were not convolved with HRF as the behavioral lag between stimulus and response was sufficient to accommodate the hemodynamic delay of the BOLD response. Pearson correlation coefficient between the ISC time series and the fear rating were then computed to reveal how across subject similarity in neural activity is associated with feelings of fear. The assumption of independence between data points in the voxel time series and the fear ratings were not met, therefore p values were calculated with a corrected degrees of freedom to account for autocorrelations in the data (Conjuring 2: 103 to 690; Insidious: 95 to 539; see Alluri et al., 2012; Pyper and Peterman, 1998), with a FDR thresholded $p = 0.001$. Dynamic ISC was chosen over the conceptually similar inter-subject phase synchronization approach (Glerean et al., 2012) as ISC provides a measure that is restricted to a specific time window irrespective of the signal phase outside of this window, whereas phase synchronization produces a measure of synchronization at each time point that nevertheless is affected by the global signal phase of the time series. ISC is therefore more suited to comparing signals across subjects who may exhibit variability in such a long global time series before performing a group level correlation with the fear rating. Note that acute fear events could not be meaningfully analyzed with ISC, as predicting the moving-averaged ISC time series with stick functions with zero duration would not be conceptually meaningful.

2.4.3. Functional connectivity analysis

Functional Connectivity was investigated by employing Seed Based Phase Synchronization (SBPS), implemented with the FunPsy toolbox (https://github.com/eglerean/funpsy) and described in detail in Glerean et al. (2012). For each participant, the demeaned BOLD time series for each voxel was band-pass filtered (0.04–0.07 Hz) using the default parameters of the FunPsy toolbox to account for cardiovascular noise, and which are necessarily strict given the long TR of the current study. Regions of interest (45 per hemisphere, 26 cerebellar) were defined based on the AAL atlas in MNI space (Tzourio-Mazoyer et al., 2002) and the BOLD signal was averaged across voxels in each region. The phase analytic signal (in radians) of the Hilbert transformed BOLD response of each region was calculated. The instantaneous angular difference between each region pair at each time point provides a model free estimation of dynamic neural synchronization between regions that maintains the temporal precision that is lost when using a sliding window analysis. The time series of neural synchronization between each pair of regions was then correlated with the fear ratings to assess how functional connectivity altered with the fear of the participant. Alpha levels were subject to FDR correction ($p = .05$ for Conjuring 2, $p = .01$ for Insidious, with the different thresholds required to yield comparably interpretable maps), using corrected degrees of freedom based on the autocorrelation between the angular difference and fear ratings (Conjuring 2: 171 to 753; Insidious: 100 to 598).

3. Results

3.1. Behavioral Data

Behavioral data (Fig. 2) revealed that both movies elicited strong subjective feelings of fear that were also varying over time. Ratings were consistent across subjects, as indicated by the high ISC of the fear time series (mean Fisher z transformed Pearson's r: Conjuring 2 = .756; Insidious = .630) and narrow mean 95% CI (Conjuring 2 = .08; Insidious =.09). Accordingly, averaged ratings provide a good model for experienced fear during the fMRI experiment. Interestingly, there were significant positive correlations between fear ratings and 95% CI and ISC for both movies (all p's < 0.001), suggesting that, as the intensity of fear increased, variability in *absolute* ratings of fear increased, but the extent to which participant's ratings followed each other (synchronized) also increased. In other words, during fearful events participants' experience of fear showed a general increase of different orders of magnitude, which also led to more similar time-locking of subjective feelings across participants. Furthermore, the 95% CI of fear ratings increased with time (Conjuring 2: $r = .205$, $p = .037$; Insidious: $r = .548$, $p = .015$) but the ISC of fear ratings did not (Conjuring 2: $r = -.074$, $p = .222$; Insidious: $r = -.117$, $p = .285$). Peaks of the self-reported fear time series were concordant with the occurrence of jump-scares (black vertical lines in Fig. 2). The fear ratings correlated negatively with luminance (The Conjuring 2: $r = -.433$, $p < .001$; Insidious: $r = -.253$, $p < .001$), and positively with sound intensity (The Conjuring 2: $r = .408$, $p < .001$; Insidious: $r = .368$, $p < .001$).

Fear ratings were correlated with global relative motion (Conjuring 2: $r = .203$, $p < .001$; Insidious: $r = .273$, $p < .001$), but not the onset of jump-scares (Conjuring 2: $r = .025$, $p = .230$; Insidious: $r = .001$, $p = .984$) (see Supplementary Analysis 4. for a full analysis). It must be noted though, that these motion parameters were regressed out of the BOLD signal during pre-processing, and further removal risks impacting on the signal component of interest.

3.2. The effect of acute transient fear on neural activity

BOLD responses to jump-scare events (joint analysis of both movies) are shown in Fig. 3. The mean ICC coefficient across the two movies was 0.65 (indicative of moderate reliability, Koo and Li, 2016). There was extensive bilateral activity in the cuneus, precuneus, lingual gyri, middle occipital gyri, and fusiform gyri. Parietal activity was observed in bilateral precentral gyrus. In the temporal lobe, bilateral activity was observed in the posterior, middle, and anterior portions of the superior temporal gyri, as well as the middle and transverse temporal gyri. Frontal activity was observed in bilateral posterior and anterior portions of the inferior frontal gyrus, and medial frontal gyrus, and the cingulate cortex

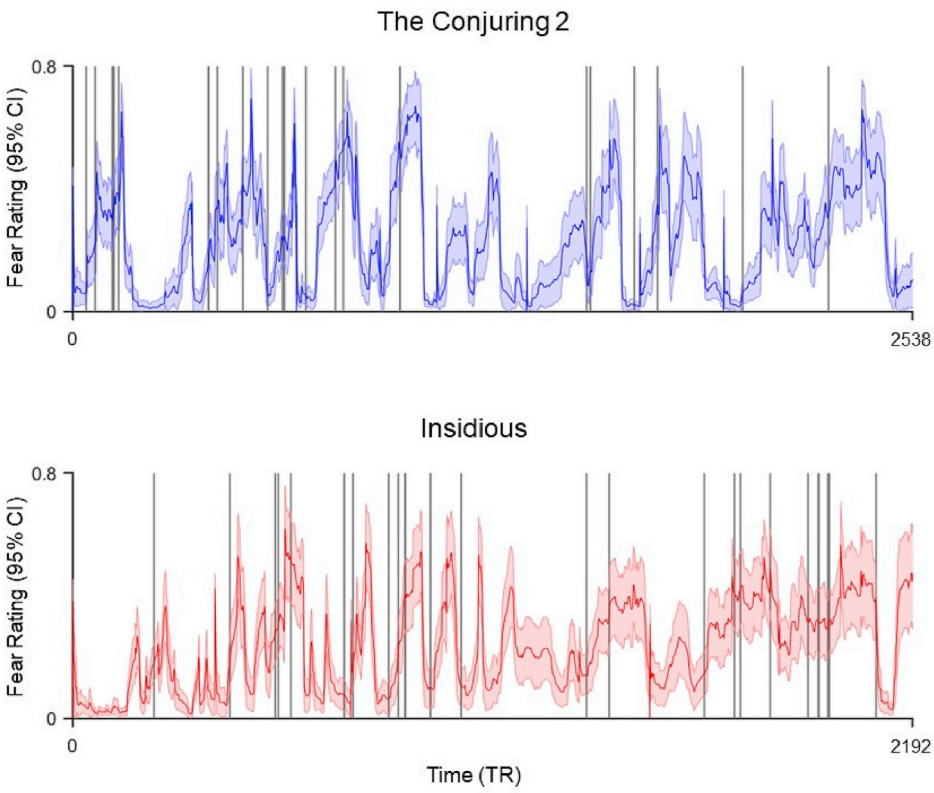

Fig. 2. Mean dynamic fear ratings with 95% confidence intervals. Black vertical lines represent the jump-scare events (Conjuring 2 n = 22; Insidious n = 24).

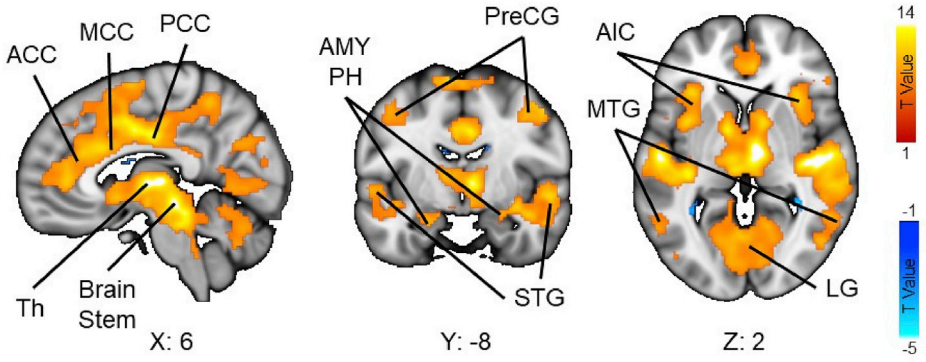

Fig. 3. The effect of acute fear (jump-scares) on neural activity collapsed across movies (FWE corrected $p = 0.001$). ACC = Anterior Cingulate Cortex, MCC = Middle Cingulate Cortex, PCC = Posterior Cingulate Cortex, Th = Thalamus, AMY = Amygdala, PH = Parrahippocampus, PreCG = PreCentral Gyrus, STG = Superior Temporal Gyrus, AIC = Anterior Insula Cortex, MTG = Middle Temporal Gyrus, LG = Lingual Gyrus. Results for each movie and the intraclass correlation analysis are in Supplementary Fig. 1.

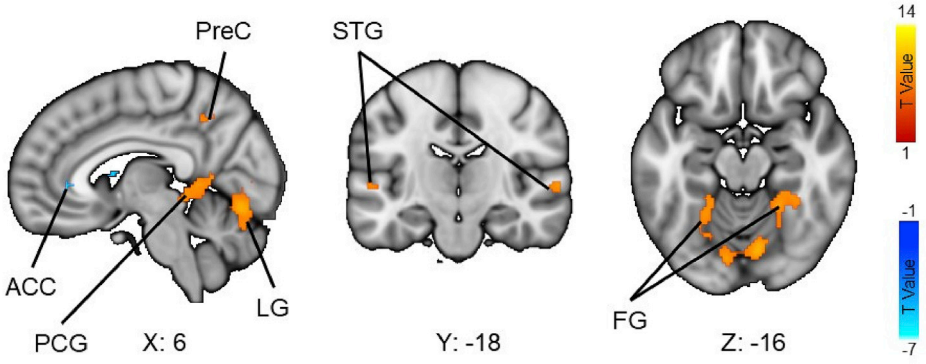

Fig. 4. The relationship between sustained fear and neural activity across both movies (FWE corrected $p = 0.001$). ACC = Anterior Cingulate Cortex, PCG = Post-Cingulate Gyrus, LG = Lingual Gyrus, PreC = Precuneus, STG = Superior Temporal Gyrus, FG = Fusiform Gyrus. Results for each movie and the intraclass correlation analysis are in Supplementary Fig. 2.

also exhibited robust activity in the anterior, middle and posterior portions. Bilateral insula cortex activity was evident in anterior and posterior regions, and also the claustrum. There was bilateral amygdala and parahippocampul activity, as well as subcortical activity in the caudate, thalamus, putamen, and the red nucleus and substania nigra of the periaqueductal gray area. A large cluster of activity was also found in the cerebellum, encompassing the cerebellar tonsil, culmen, declive, pyramis, nodule, uvula, fastigium, and cerebellar lingula. No regions showed a decrease in activity in response to the jump-scares after FWE correction. However, with an uncorrected threshold of $p < .001$, small bilateral clusters in the posterior anterior cingulate cortex, parahippocampus, and caudate were evident.

3.3. The effect of sustained fear on neural activity

Regions that exhibited activity significantly correlated with the sustained level of fear are shown in Fig. 4. The mean ICC coefficient across movies was 0.61 (indicative of moderate reliability, Koo and Li, 2016). Fear was associated with activity in bilateral posterior middle occipital gyri, left fusiform gyri, and cuneus, and also the right lingual gyrus and right precuneus. Cerebellar activity was evident in left uvula, and bilateral declive, culmen, and pyramis. No regions exhibited a negative relationship with fear at a FWE corrected threshold of $p <. 001$. However, at a FWE corrected threshold of $p < .05$, decreased activity was observed in bilateral post-central gyrus, and bilateral inferior parietal lobe extending to the supramarginal gyrus in the left hemisphere. In the frontal lobe, there was activity in the left ventral and dorsal inferior frontal gyri, left ventral medial frontal gyrus, left ventral and dorsal middle frontal gyrus, left precentreal gyrus, and bilateral medial frontal gyri. Regions of the insular cortex (left anterior and right middle) also exhibited decreased activity with rising fear, as did the left claustrum, and decreases in activity were also observed in bilateral parrahippocampus, caudate, and thalamus. When luminance and sound intensity were added as nuisance regressors (Supplementary Fig. 3A), the activity of the posterior cingulate cortex, lingual gyrus, and parrahippocampul gyrus remained, suggesting these regions to be sensitive to the fear experienced, whereas the activity of the superior temporal gyrus and precuneus were absent, suggesting that the response of these regions was driven by stimulus features such as intense sounds and diminished/uncertain visual input that contribute to the experience of fear. The pattern of negative associations with fear was more stable after accounting for luminance and sound intensity (bilateral posterior superior temporal gyri, left precentral gyrus, left dorsal inferior frontal gyrus, right dorsal superior frontal gyrus, bilateral anterior insula cortex, bilateral anterior cingulate cortex, and caudate).

3.4. The effect of sustained fear on intersubject synchronization of brain activity (ISC)

Mean ISC maps for each movie are shown in Fig. 5. For both movies, synchronized activity was evident across the whole brain, but there was a clear gradient from higher synchronization in the sensory cortices to parietal areas and association cortices, to the lowest synchronization in frontal regions.

The relationship between the dynamic ISC and the sustained fear is depicted in Fig. 6. Intensity of fear was associated with increased ISC as the level of fear rose in a large bilateral swathe of cortex from the anterior and middle portions of the cingulate gyrus, to the medial frontal gyrus and paracentral lobule, to the primary somatosensory cortex (postcentral gyrus) and the adjacent precentral gyri. This effect was evident in both movies. Replicable effects were also found in the left superior frontal gyrus (also right hemisphere for The Conjuring 2), bilateral inferior frontal gyri, bilateral posterior, middle and anterior insula cortices, and bilateral thalamus. Both movies exhibited a fear dependent increase in ISC in posterior nodes of the frontoparietal attention circuits (bilateral inferior parietal cortices) and precuneus, the temporal lobe (right

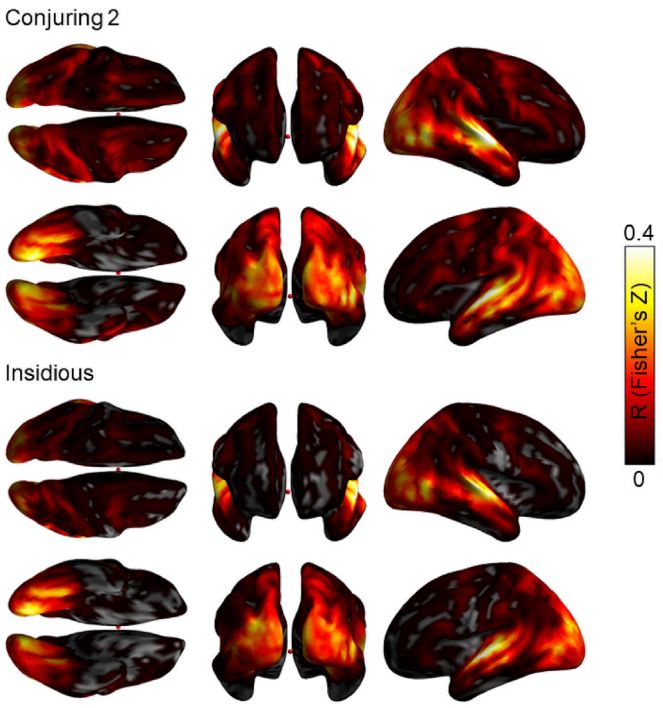

Fig. 5. Intersubject Correlation Maps. Voxel intensities show mean Fisher z transformed Pearson's correlation coefficient for each subject pair's voxel-wise time series across the whole movie. Statistical significance of the ISC values was calculated by means of a fully nonparametric voxel wise permutation test of the r value (1,000,000 realizations, FDR corrected $p = 0.05$).

anterior superior temporal gyrus, bilateral middle temporal gyrus), and occipital lobe (left post cingulate gyrus for both movies, right post-cingulate gyrus). The fear related increase in ISC was also evident in the cerebellum for both movies (culmen, bilateral tuber, pyramis, devlice and inferior semi-lunar lobe). When low-level stimulus features were entered as a covariate, the pattern of activity remained essentially the same, except for an absence of activity in the superior temporal gyrus (Supplementary Fig. 3B).

Despite the consistent effects across both movies, some differences were also observed. The Conjuring 2 exhibited increased ISC as fear increased in the left cuneus, bilateral superior parietal lobe and, in the cerebellum, the cerebellar lingual and tonsil and uvula. The Conjuring 2 also exhibited several regions in the occipital lobe that showed a decrease in the ISC as fear increased, albeit with a lower FDR corrected threshold of $p = .05$ (bilateral middle occipital gyri and bilateral lingual gyri). Insidious exhibited additional positive fear related ISC in frontal regions (bilateral anterior medial frontal gyrus and middle frontal gyri), temporal regions (left anterior superior temporal gyrus, bilateral posterior superior temporal sulcus and right uncus), and occipital regions (bilateral superior occipital gyri). No negative associations were observed for Insidious.

Fear-dependent changes in functional connectivity (Seed Based Phase Synchronization) The relationship between fear ratings and SBPS elicited a dense network of connections (Fig. 7) that contrast starkly with the discrete networks identified in response to just acute or sustained fear. Fear correlated with widespread functional connectivity across the brain for both movies, and several regions exhibited consistently high number of connections, although these results were stronger for Insidious (FDR correct $p = .01$) than Conjuring 2 (FDR corrected $p = .05$). These connectivity changes were also consistent across movies: the mean ICC coefficient for the unthresholded connectivity matrices across the two movies was 0.95 (indicative of excellent reliability, Koo and Li, 2016). Fear related connectivity within the frontal cortex was sparse, except for the precentral gyri, which acted as a hub for fear relevant connectivity with many areas within the frontal cortex. The right frontal middle gyrus

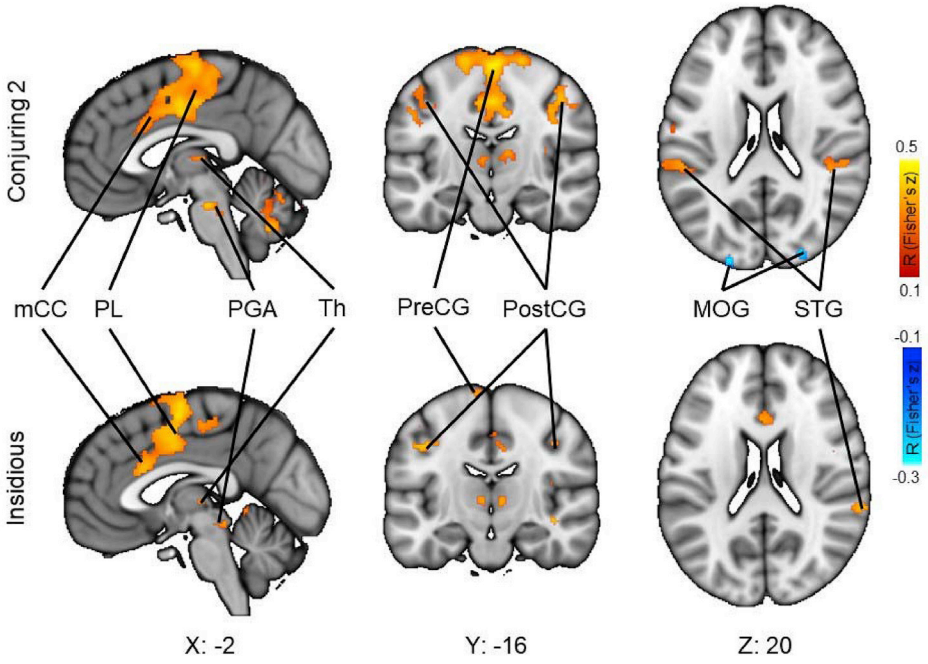

Fig. 6. Fear-dependent dynamic inter-subject neural synchronization for The Conjuring 2 (top) and Insidious (bottom). The data are shown as Fisher z-transformed Pearson's r (FDR corrected $p = .001$). mCC = Middle Cingulate Cortex, PL = Paracentral Lobule, PGA = Periaqueductal Gray Area, Th = Thalamus, PreCG = Pre-Central Gyrus, Post CG = PostCentral Gyrus, MOG = Middle Occipital Gyrus, STG = Superior Temporal Gyrus.

exhibited increased functional connectivity with many regions in the occipital cortex, as well as the temporal and parietal cortices. The left postcentral gyrus increased fear related functional connectivity with several regions in the frontal lobe, and the cingulate cortex, which itself acted as a hub increasing connectivity with the temporal lobe and the limbic system as fear increased. Fear was associated with functional connectivity between left paracentral lobule and several regions in the frontal lobe, cingulate cortex, and posterior central gyrus. There were additional highly connected regions for each individual movie. The Conjuring 2 elicited increased connectivity as fear increased between the right frontal inferior orbital gyrus and the temporal lobe, of which the left superior temporal gyrus connected richly with the limbic system, whilst the left middle temporal lobe connected richly with the frontal lobe. The left middle frontal orbital gyrus in turn exhibited multiple connections with the temporal lobe. For Insidious, several frontal gyri (right inferior operculum, right inferior triangularis, right superior medial, left inferior orbital) exhibited fear associated connectivity with occipital and parietal regions, subcortical regions, and the cerebellum. Bilateral insula cortices increased connectivity with frontal and cingulate cortices, as well as the cerebellum. Bilateral transverse temporal gyri connected richly with anterior cingulate cortex, whilst in the partial lobe, the right supra-marginal gyrus, right inferior parietal lobe, and bilateral postcentral gyri increased connectivity with frontal, cingulate, and occipital regions.

4. Discussion

Our main finding was that acute fear elicited consistent activity in a distributed set of cortical, limbic, and cerebellar regions, most notably the prefrontal cortex, paracentral lobule, amygdala, cingulate cortex, insula, PAG, parrahippocampus, and thalamus. These regions have been previously identified as being active in response to threat (Mobbs et al., 2007; Qi et al., 2018; Zhu and Thagard, 2002). However, the activity of these regions was not associated with slower-frequency experience of sustained fear, despite the high pass filter of 256s optimizing the GLM analysis to detect the low energy changes in fear ratings, which peaked at around 0.01 Hz. Instead, sustained fear ratings were associated with increased activity in the sensory (both auditory and visual) cortices and a small portion of the parietal lobule. These differential patterns of activity were confirmed by directly contrasting neural activity in response to sustained fear immediately before threat onset, with that immediately after threat onset (Supplementary Analysis 1). These results suggest separable mechanisms for sustained fear involved in the pre-encounter anticipation of threat, requiring increased perceptual and attentional focus, and reactionary responses to acute threat onset, requiring instinctive emotional processing centers, learning/memory, and action planning processes. Importantly, these effects were replicable in two independent samples of subjects and with two different stimulus movies, highlighting the replicability and generalizability of the results.

4.1. Different timescales of fear

As fear becomes more imminent, amplified sensory processing and vigilance promote evidence gathering, whilst motor preparation (evidenced by activation in the precentral gyrus) promotes rapid protective responses whenever needed. The sudden onset of threat in turn elicits an abrupt increase in activity in several regions, notably the amygdala, PGA, and the hippocampus. The thalamus may act as a relay between these areas and cortical regions of the insula cortex, the anterior and posterior cingulate cortices, and the precentral gyrus.

Interestingly, brain regions associated with the onset of acute fearful stimuli, despite not being associated with increasing fear at the individual level, did exhibit significant fear-dependent intersubject synchronization. That is, during high-fear episodes, brain activity became time-locked across subjects in several brain regions associated with the rapid onset of threat, notably the PGA, the cingulate cortex, and paracentral lobule. It is thus possible that sustained fear induces a reliable time-locked fluctuation in these regions, possibly reflecting the role that a commonly experienced emotional response has in regions associated with emotional experience and action planning. Importantly, this increased similarity at the neural level was also associated with increased similarity in behavioral measures of fear: The more afraid the participants felt, the more similar their subjective feeling time courses became. This parallels with behavioral work showing that negative emotional states are associated with narrowing of mental focus and cognitive

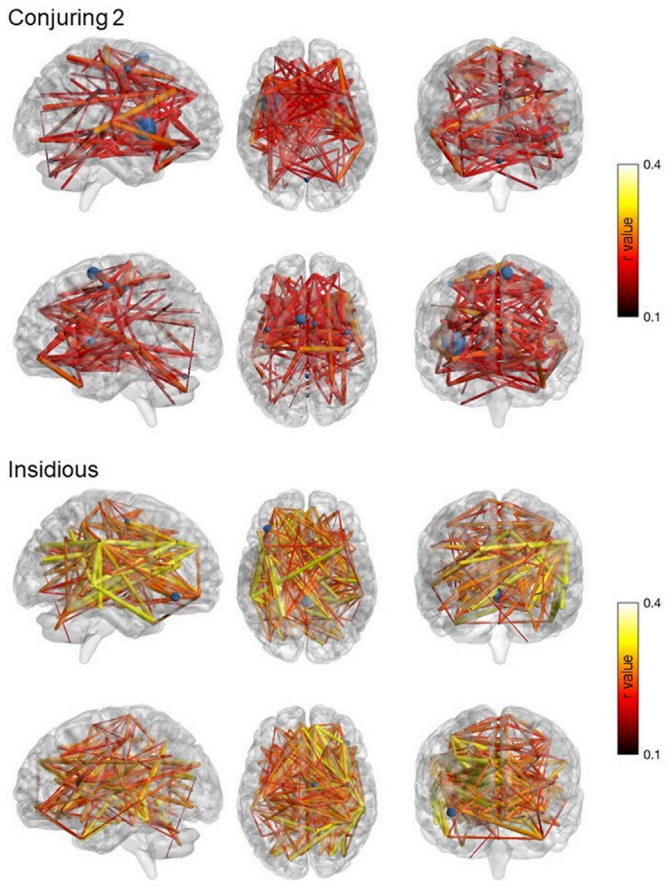

Fig. 7. Seed-Based Phase Synchronization for each movie. Conjuring 2 (top, FDR corrected $p = 0.05$) and Insidious (bottom, FDR corrected $p = 0.01$). Phase similarity at each time point was calculated for each of 166 ROI pairs taken from the AAL atlas and correlated with the fear ratings. Connectome graphs (BrainNet Viewer: Xia, Wang and He, 2013) depict those region pairs that exhibited a significant relationship between phase similarity and fear ratings with node size reflecting the number of connections and edge size and color reflecting the strength of the correlation. See Supplementary Figs. 4 and 5 for a depiction of these results as correlation matrices.

processing styles (Bishop, 2007; Panksepp, 1998).

4.2. Functional networks for the fear response

Functional connectivity analysis revealed that, despite regional responses to sustained fear being modest, fear was associated with profound functional connectivity changes. This functional connectivity increased as fear increased, as if the sustained anticipatory fear mechanism prepared the reactionary acute fear mechanism as threat became closer in spatiotemporal proximity. The frontal cortex exhibited increased connectivity with not only visual processing areas of the occipital cortex, but emotional processing areas of the limbic system, of which the amygdala has previously been shown to exhibit within-region connectivity during heightened fear states (Kinreich et al., 2011). The frontal lobe and cingulate cortex, both implicated in emotional experience (Etkin et al., 2011), exhibited fear related connectivity with the motor regions such as the pre and post central gyri. This suggests that, although networks involved in sustained and acute fear may be dissociable in terms of absolute neural activity, they exhibit increasingly correlated activity during threatening situations.

We propose that sensory and motor areas act as an anticipatory fear network that serves to resolve ambiguity, increase vigilance, and appraise the emotional content of sensory information and prepares avoidance related behavior. The sudden onset of threat, however, elicits abrupt activity in regions involved not only in emotional experience (Critchley, 2005; Phan et al., 2002), but also in processing the saliency and arousal of the stimulus (Liberzon et al., 2003; Satpute et al., 2013), memory processes (Phelps, 2004), and the planning of rapid responses to mitigate danger (Beckmann et al., 2009). This reactionary network nevertheless exhibits increasingly synchronized activity between individuals as anticipatory fear increases, prior to threat onset. Moreover, this sustained fear was associated with increasing functional connectivity between these networks as if anticipatory processes were priming reactionary processes as threat becomes more likely and the need for immediate action becomes more prescient (Fanselow, 1994; Lang et al., 2000; Lehne and Koelsch, 2015), and also regions implicated in threat appraisal and decision making (Kalisch and Gerlicher, 2014; Rushworth et al., 2007). However, although sustained fear precipitated widespread connectivity throughout the brain, the effect of fear on the synchronization of this connectivity across individuals (Inter-subject Seed Based Phase Synchronization, Glerean et al., 2012; Simony et al., 2016, see Supplementary Analysis 2) was far more limited and restricted to activity between regions implicated in the anticipation and response to threat itself. That is, the connectivity became increasingly time locked between regions associated with visual and emotional processing, and action planning and preparation. This suggests that fear not only synchronizes neural activity in these regions across individuals, but also the functional connectivity between these regions as the preparation to respond becomes increasingly similar.

Altogether our results establish that networks involved in sustained fear during an anticipatory pre-encounter phase of threat monitoring and acute fear as a reaction to threat onset do not work in isolation that require a qualitative shift depending on a discrete threshold of threat proximity. Instead, they work in concert throughout threat evaluation that gradually shifts from one to the other as threat increases in proximity. This insight would not have been possible using conventional model based approaches that require controlled stimuli discretely categorized into anticipatory and reactionary stimuli, and which would inevitably lead to the description of a binary system of pre and post threat onset (e.g., Mobbs et al., 2007; Qi et al., 2018). Instead, using naturalistic stimuli and a data driven approach that permits the reliability of neural activity to be established whilst accommodating the complex and dynamic nature of the neural signal and the realistic stimuli that elicits it (Glerean et al., 2012; Hasson et al., 2004), we were nevertheless able to not only confirm these systems, but reveal how they functionally interact during a fearful situation.

5. Conclusions

Our combination of model-based and model-free approaches for naturalistic neuroimaging data reveals dynamic interaction between two separable systems for the anticipation of threat from environmental cues, and the reaction to threat onset, with a temporal shift between them as the spatiotemporal proximity of threat decreases, and anticipatory planning mechanisms inform subsequent responses. These effects are reliable across subjects and experimental conditions, further highlighting the feasibility of naturalistic stimulation models in understanding brain basis of emotions.

Funding

The research was funded by grants awarded to LN from the Academy of Finland (#294897) and a European Research Council Starting Grant (#313000).

Declaration of competing interest

The authors declare no competing interests.

CRediT authorship contribution statement

Matthew Hudson: Conceptualization, Methodology, Software, Validation, Formal analysis, Investigation, Data curation, Writing - original draft, Writing - review & editing, Visualization. **Kerttu Seppälä:** Investigation, Writing - review & editing. **Vesa Putkinen:** Investigation, Writing - review & editing. **Lihua Sun:** Investigation, Writing - review & editing. **Enrico Glerean:** Methodology, Software, Formal analysis, Writing - review & editing. **Tomi Karjalainen:** Methodology, Software, Investigation, Writing - review & editing. **Henry K. Karlsson:** Investigation. **Jussi Hirvonen:** Investigation. **Lauri Nummenmaa:** Conceptualization, Methodology, Writing - original draft, Writing - review & editing, Supervision, Project administration, Funding acquisition.

Appendix A. Supplementary data

Supplementary data to this article can be found online at https://doi.org/10.1016/j.neuroimage.2020.116522.

References

Adolphs, R., Nummenmaa, L., Todorov, A., Haxby, J.V., 2016. Data-driven approaches in the investigation of social perception, 371. Philosphical Transactions of the Royal Society of London Series B. https://doi.org/10.1098/rstb.2015.0367.

Alluri, V., Toiviainen, P., Jääskeläinen, I.P., Glerean, E., Sams, M., Brattico, E., 2012. Large-scale brain networks emerge from dynamic processing of musical timbre, key and rhythm. Neuroimage 59, 3677–3689. https://doi.org/10.1016/j.neuroimage.2011.11.019.

Beckmann, M., Johansen-Berg, H., Rushworth, M.F.S., 2009. Connectivity-based parcellation of human cingulate cortex and its relation to functional specialization. J. Neurosci. 29, 1175–1190. https://doi.org/10.1523/JNEUROSCI.3328-08.2009.

Belitski, A., Gretton, A., Magri, C., Murayama, Y., Montemurro, M.A., Logothetis, N.K., Panzeri, S., 2008. Low-frequency local field potentials and spikes in primary visual cortex convey independent visual information. J. Neurosci. 28, 5696–5709. https://doi.org/10.1523/JNEUROSCI.0009-08.2008.

Bennett, C.M., Miller, M.B., 2010. How reliable are the results from functional magnetic resonance imaging? Ann. N. Y. Acad. Sci. 1191, 133–155. https://doi.org/10.1111/j.1749-6632.2010.05446.x.

Bernhardt, B.C., Singer, T., 2012. The neural basis of empathy. Annu. Rev. Neurosci. 35, 1–23. https://doi.org/10.1146/annurev-neuro-062111-150536.

Bishop, S.J., 2007. Neurocognitive mechanisms of anxiety: an integrative account. Trends Cogn. Sci. 11, 307–316. https://doi.org/10.1016/j.tics.2007.05.008.

Chen, G., Taylor, P.A., Haller, S.P., Kircanski, K., Stoddard, J., Pine, D.S., Leibenluft, E., Brotman, M.A., Cox, R.W., 2017. Intraclass correlation: improved modelling approaches and applications for neuroimaging. Hum. Brain Mapp. 39, 1187–1206. https://doi.org/10.1002/hbm.23909.

Critchley, H.D., 2005. Neural mechanisms of autonomic, affective, and cognitive integration. J. Comp. Neurol. 493, 154–166. https://doi.org/10.1002/cne.20749.

Critchley, H.D., Mathias, C.J., Dolan, R.J., 2002. Fear conditioning in humans: the influence of awareness and autonomic arousal on functional neuroanatomy. Neuron 33, 653–663. https://doi.org/10.1016/s0896-6273(02)00588-3.

Çukur, T., Nishimoto, S., Huth, A.G., Gallant, J.L., 2013. Attention during natural vision warps semantic representation across the human brain. Nat. Neurosci. 16, 763–770. https://doi.org/10.1038/nn.3381.

Ekman, P., 1992. An argument for basic emotions. Cognit. Emot. 6, 169–200. https://doi.org/10.1080/02699939208411068.

Eryilmaz, H., Van De Ville, D., Schwartz, S., Vuilleumier, P., 2011. Impact of transient emotions on functional connectivity during subsequent resting state: a wavelet correlation approach. Neuroimage 54, 2481–2491. https://doi.org/10.1016/j.neuroimage.2010.10.021.

Etkin, A., Egner, T., Kalisch, R., 2011. Emotional processing in anterior cingulate and medial prefrontal cortex. Trends Cogn. Sci. 15, 85–93. https://doi.org/10.1016/j.tics.2010.11.004.

Fanselow, M.S., 1994. Neural organization of the defensive behavior system responsible for fear. Psychon. Bull. Rev. 1, 429–438. https://doi.org/10.3758/BF03210947.

Felsen, G., Dan, Y., 2005. A natural approach to studying vision. Nat. Neurosci. 8, 1643–1646. https://doi.org/10.1038/nn1608.

Finucane, A.M., 2011. The effect of fear and anger on selective attention. Emotion 11, 970–974. https://doi.org/10.1037/a0022574.

Fox, C.J., Iaria, G., Barton, J.J.S., 2009. Defining the face processing network: optimization of the functional localizer in fMRI. Hum. Brain Mapp. 30, 1637–1651. https://doi.org/10.1002/hbm.20630.

Glerean, E., Salmi, J., Lahnakoski, J.M., Jääskeläinen, I.P., Sams, M., 2012. Functional magnetic resonance imaging phase synchronization as a measure of dynamic functional connectivity. Brain Connect. 2, 91–101. https://doi.org/10.1089/brain.2011.0068.

Hasson, U., Nir, Y., Levy, I., Fuhrmann, G., Malach, R., 2004. Intersubject synchronization of cortical activity during natural vision. Science 303, 1634–1640. https://doi.org/10.1126/science.1089506.

Hasson, U., Furman, O., Clark, D., Dudai, Y., Davachi, L., 2008. Enhanced intersubject correlations during movie viewing correlate with successful episodic encoding. Neuron 57, 452–462. https://doi.org/10.1016/j.neuron.2007.12.009.

Jump, 2017, February 1st. Where's the Jump? Retrieved from. https://wheresthejump.com/.

Kalisch, R., Gerlicher, A.M.V., 2014. Making a mountain out of a molehill: on the role of the rostral dorsal anterior cingulate and dorsomedial prefrontal cortex in conscious threat appraisal, catastrophizing, and worrying. Neurosci. Biobehav. Rev. 42, 1–8. https://doi.org/10.1016/j.neubiorev.2014.02.002.

Kauppi, J.-P., Pajula, J., Tohka, J., 2014. A versatile software package for inter-subject correlation based analyses of fMRI. Front. Neuroinf. 8, 1–13. https://doi.org/10.3389/fninf.2014.00002.

Kinreich, S., Intrator, N., Hendler, T., 2011. Functional cliques in the amygdala and related brain networks drivin by fear assessment acquired during movie viewing. Brain Connect. 1, 484–495. https://doi.org/10.1089/brain.2011.0061.

Knight, D.C., Smith, C.N., Cheng, D.T., Stein, E.A., Helmstetter, F.J., 2004. Amygdala and hippocampal activity during acquisition and extinction of human fear conditioning. Cognit. Affect Behav. Neurosci. 4, 317–325. https://doi.org/10.3758/CABN.4.3.317.

Koo, T.K., Li, M.Y., 2016. A guideline of selecting and reporting intraclass correlation coefficients for reliability research. J. Chiropr. Med. 15, 155–163. https://doi.org/10.1016/j.jcm.2016.02.012.

Kreibig, S.D., 2010. Autonomic nervous system activity in emotion: a review. Biol. Psychiatry 84, 394–421. https://doi.org/10.1016/j.biopsycho.2010.03.010.

LaBar, K.S., Gatenby, J.C., Gore, J.C., LeDoux, J.E., Phelps, E.A., 1998. Human amygdala activation during conditioned fear acquisition and extinction: a mixed-trial fMRI study. Neuron 20, 937–945. https://doi.org/10.1016/S0896-6273(00)80475-4.

Lahnakoski, J.M., Glerean, E., Jääskeläinen, I.P., Hyönä, J., Hari, R., Sams, M., Nummenmaa, L., 2014. Synchronous brain activity across individuals underlies shared psychological perspectives. Neuroimage 100, 316–324. https://doi.org/10.1016/j.neuroimage.2014.06.022.

Lang, P.J., Davis, M., Öhman, A., 2000. Fear and anxiety: animal models and human cognitive psychophysiology. J. Affect. Disord. 61, 137–159. https://doi.org/10.1016/s0165-0327(00)00343-8.

Lehne, M., Koelsch, S., 2015. Toward a general psychological model of tension and suspense. Front. Psychol. 6, 1–11. https://doi.org/10.3389/fpsyg.2015.00079.

Liberzon, I., Phan, K.L., Decker, L.R., Taylor, S.F., 2003. Extended amygdala and emotional salience: a PET activation study of positive and negative affect. Neuropsychopharmacology 28, 726–733. https://doi.org/10.1038/sj.npp.1300113.

Lissek, S., Bradford, D.E., Alvarez, R.P., Burton, P., Espensen-Sturges, T., Reynolds, R.C., Grillon, C., 2014. Neural substrates of classically conditioned fear-generalization in humans: a parametric fMRI study. Soc. Cogn. Affect. Neurosci. 9, 1134–1142. https://doi.org/10.1093/scan/nst096.

Milad, M.R., Quirk, G.J., Pitman, R.K., Orr, S.P., Fischl, B., Rauch, S.L., 2007. A role for the human dorsal anterior cingulate cortex in fear expression. Biol. Psychiatry 62, 1191–1194. https://doi.org/10.1016/j.biopsych.2007.04.032.

Mobbs, D., Petrovic, P., Marchant, J.L., Hassabis, D., Weiskopf, N., Seymour, B., Dolan, R.J., Frith, C.D., 2007. When fear is near: threat imminence elicits prefrontal-periaqueductal gray shifts in humans. Science 317, 1079–1083. https://doi.org/10.1126/science.1144298.

Morris, J.S., Buchel, C., Dolan, R.J., 2001. Parallel neural responses in amygdala subregions and sensory cortex during implicit fear conditioning. Neuroimage 13, 1044–1052. https://doi.org/10.1006/nimg.2000.0721.

Nummenmaa, L., Saarimäki, H., 2017. Emotions as discrete patterns of systemic activity. Neurosci. Lett. 693, 3–8. https://doi.org/10.1016/j.neulet.2017.07.012.

Nummenmaa, L., Glerean, E., Viinikainen, M., Jääskeläinen, I.P., Hari, R., Sams, M., 2012. Emotions promote social interaction by synchronizing brain activity across individuals. Proc. Natl. Acad. Sci. U. S. A. 109, 9599–9604. https://doi.org/10.1073/pnas.1206095109.

Nummenmaa, L., Glerean, E., Hari, R., Hietanen, J.K., 2014a. Bodily maps of emotions. Proc. Natl. Acad. Sci. U. S. A. 111, 646–651. https://doi.org/10.1073/pnas.1321664111.

Nummenmaa, L., Saarimäki, H., Glerean, E., Gotsopoulos, A., Jääskeläinen, I.P., Hari, R., Sams, M., 2014b. Emotional speech synchronizes brains across listeners and engages large-scale dynamic brain networks. Neuroimage 102, 498–509. https://doi.org/10.1016/j.neuroimage.2014.07.063.

Nummenmaa, L., Hari, R., Hietanen, J.K., Glerean, E., 2018a. Maps of subjective feelings. Proc. Natl. Acad. Sci. U. S. A. 115, 9198–9203. https://doi.org/10.1073/pnas.1807390115.

Nummenmaa, L., Lahnakoski, J.M., Glerean, E., 2018b. Sharing the social world via intersubject neural synchronisation. Curr. Opin. Psychol. 24, 7–14. https://doi.org/10.1016/j.copsyc.2018.02.021.

Öhman, A., Mineka, S., 2001. Fears, phobias, and preparedness: toward an evolved model of fear and fear learning. Psychol. Rev. 108, 483–522. https://doi.org/10.1037//0033-295X.108.3.483.

Öhman, A., Flykt, A., Esteves, F., 2001. Emotion drives attention: detecting the snake in the grass. J. Exp. Psychol. Gen. 130, 466–478. https://doi.org/10.1037//0096-3445.130.3.466.

Pajula, J., Tohka, J., 2014. Effects of spatial smoothing on inter-subject correlation based analysis of FMRI. Magn. Reson. Imag. 32, 1114–1124. https://doi.org/10.1016/j.mri.2014.06.001.

Panksepp, J., 1982. Toward a general psychobiological theory of emotions. Behav. Brain Sci. 5, 407–467. https://doi.org/10.1017/S0140525X00012759.

Panksepp, J., 1998. Affective Neuroscience: the Foundations of Human and Animal Emotions. Oxford University Press, Oxford.

Passamonti, L., Rowe, J.B., Ewbank, M., Hampshire, A., Keane, J., Calder, A.J., 2008. Connectivity from the ventral anterior cingulate to the amygdala is modulated by

appetitive motivation in response to facial signals of aggression. Neuroimage 43, 562–570. https://doi.org/10.1016/j.neuroimage.2008.07.045.
Phan, K.L., Wager, T., Taylor, S.F., Liberzon, I., 2002. Functional neuroanatomy of emotion: a meta-analysis of emotion activation studies in PET and fMRI. Neuroimage 16, 331–348. https://doi.org/10.1006/nimg.2002.1087.
Phelps, E.A., 2004. Human emotion and memory: interactions of the amygdala and hippocampal complex. Curr. Opin. Neurobiol. 14, 198–202. https://doi.org/10.1016/j.conb.2004.03.015.
Ploghaus, A., Tracey, I., Gati, J.S., Clare, S., Menon, R.S., Matthews, P.M., Rawlins, N.P., 1999. Dissociating pain from its anticipation in the human brain. Science 284, 1979–1981. https://doi.org/10.1126/science.284.5422.1979.
Power, J.D., Mitra, A., Laumann, T.O., Snyder, A.Z., Schlaggar, B.L., Petersen, S.E., 2012. Methods to detect, characterize, and remove motion artifact in resting state fMRI. Neuroimage 84, 320–341. https://doi.org/10.1016/j.neuroimage.2013.08.
Pyper, B.J., Peterman, R.M., 1998. Comparison of methods to account for autocorrelation in correlation analyses of fish data. Can. J. Fish. Aquat. Sci. 55, 2127–2140. https://doi.org/10.1139/f98-104.
Qi, S., Hassabis, D., Sun, J., Guo, F., Daw, F., Mobbs, D., 2018. How cognitive and reactive fear circuits optimize escape decisions in humans. Proc. Natl. Acad. Sci. U. S. A. 115, 3186–3191. https://doi.org/10.1073/pnas.1712314115.
Rodrigues, S.M., LeDoux, J.E., Sapolsky, R.M., 2009. The Influence of Stress Hormones on Fear Circuitry. Annual Review of Neuroscience 32, 289–313. https://doi.org/10.1146/annurev.neuro.051508.135620.
Rushworth, M.F.S., Buckley, M.J., Behrens, T.E.J., Walton, M.E., Bannerman, D.M., 2007. Functional organization of the medial frontal cortex. Curr. Opin. Neurobiol. 17, 220–227. https://doi.org/10.1016/j.conb.2007.03.001.
Saarimäki, H., Gostopoulos, A., Jääskeläinen, I.P., Lampinen, J., Vuilleumier, P., Hari, R., Sams, M., Nummenmaa, L., 2016. Discrete neural signatures of basic emotions. Cerebr. Cortex 6, 2563–2573. https://doi.org/10.1093/cercor/bhv086.
Satpute, A.B., Wager, T.D., Cohen-Adad, J., Bianciardi, M., Choi, J.-K., Buhle, J.T., Wald, L.L., Barretta, L.F., 2013. Identification of discrete functional subregions of the human periaqueductal gray. Proc. Natl. Acad. Sci. U. S. A. 110, 17101–17106. https://doi.org/10.1073/pnas.1306095110.
Schultz, J., Brockhaus, M., Bulthoff, H.H., Pilz, K.S., 2013. What the human brain likes about facial motion. Cerebr. Cortex 23, 1167–1178. https://doi.org/10.1093/cercor/bhs106.
Shrout, P.E., Fleiss, J.L., 1979. Intraclass correlations: uses in assessing rater reliability. Psychol. Bull. 86, 420–428. https://doi.org/10.1037/0033-2909.86.2.420.
Simony, E., Honey, C.J., Chen, J., Lositsky, O., Yeshurun, Y., Wiesel, A., Hasson, U., 2016. Dynamic reconfiguration of the default mode network during narrative comprehension. Nat. Commun. 7, 1–13. https://doi.org/10.1038/ncomms12141.
Smirnov, D., Saarimäki, H., Glerean, E., Hari, R., Sams, M., Nummenmaa, L., 2019. Emotions amplify speaker-listener neural alignment. Hum. Brain Mapp. 40, 4777–4788. https://doi.org/10.1002/hbm.24736.
Smith, M.L., Cottrell, G.W., Gosselin, F., Schyns, P.G., 2005. Transmitting and decoding facial expressions. Psychol. Sci. 16, 184–189. https://doi.org/10.1111/j.0956-7976.2005.00801.x.
Tettamanti, M., Rognoni, E., Cafiero, R., Costa, T., Galati, D., Perani, D., 2012. Distinct pathways of neural coupling for different basic emotions. Neuroimage 59, 1804–1817. https://doi.org/10.1016/j.neuroimage.2011.08.018.
Touryan, J., Felsen, G., Dan, Y., 2005. Spatial structure of complex cell receptive fields measured with natural images. Neuron 45, 781–791. https://doi.org/10.1016/j.neuron.2005.01.029.
Tzourio-Mazoyer, N., Landeau, B., Papathanassiou, D., Crivello, F., Etard, O., Delcroix, N., Mazoyer, B., Joliot, M., 2002. Automated anatomical labelling of activations in SPM using a macroscopic anatomical parcellation of the MNI MRI single-subject brain. Neuroimage 15, 273–289. https://doi.org/10.1006/nimg.2001.0978.
Volynets, S., Glerean, E., Hietanen, J., Hari, R., Nummenmaa, L., 2019. Bodily maps of emotions are culturally universal. Emotion. https://doi.org/10.1037/emo0000624. In press.
Xia, M., Wang, J., He, Y., 2013. BrainNet viewer: a network visualization tool for human brain connectomics. PLoS One 8, e68910. https://doi.org/10.1371/journal.pone.0068910.
Zhu, J., Thagard, P., 2002. Emotion and action. Philos. Psychol. 15, 19–36. https://doi.org/10.1080/09515080120109397.